

# Jasmonate-Responsive ERF Transcription Factors Regulate Steroidal Glycoalkaloid Biosynthesis in Tomato

Chonprakun Thagun<sup>1</sup>, Shunsuke Imanishi<sup>2</sup>, Toru Kudo<sup>3</sup>, Ryo Nakabayashi<sup>4</sup>, Kiyoshi Ohyama<sup>5</sup>, Tetsuya Mori<sup>4</sup>, Koichi Kawamoto<sup>6</sup>, Yukino Nakamura<sup>3</sup>, Minami Katayama<sup>3</sup>, Satoko Nonaka<sup>6</sup>, Chiaki Matsukura<sup>6</sup>, Kentaro Yano<sup>3</sup>, Hiroshi Ezura<sup>6</sup>, Kazuki Saito<sup>4,7</sup>, Takashi Hashimoto<sup>1</sup> and Tsubasa Shoji<sup>1,\*</sup>

<sup>1</sup>Graduate School of Biological Sciences, Nara Institute of Science and Technology, Ikoma, 630-0101 Japan

<sup>2</sup>Institute of Vegetable and Tea Science, National Agriculture and Food Research Organization, Tsu, 514-2392 Japan

<sup>3</sup>Department of Life Sciences, School of Agriculture, Meiji University, Kawasaki, 214-8571 Japan

<sup>4</sup>RIKEN Center for Sustainable Resource Science, Yokohama, 230-0045 Japan

<sup>5</sup>Department of Chemistry and Materials Science, Tokyo Institute of Technology, Meguro-ku, 152-8551 Japan

<sup>6</sup>Graduate School of Life and Environmental Sciences, University of Tsukuba, Tsukuba, 305-8577 Japan

<sup>7</sup>Graduate School of Pharmaceutical Sciences, Chiba University, Chiba, 260-8675 Japan

\*Corresponding author: E-mail, t-shouji@bs.naist.jp; Fax, +81-743-72-5529.

(Received March 6, 2016; Accepted March 23, 2016)

**Steroidal glycoalkaloids (SGAs) are cholesterol-derived specialized metabolites produced in species of the Solanaceae. Here, we report that a group of jasmonate-responsive transcription factors of the ETHYLENE RESPONSE FACTOR (ERF) family (JREs) are close homologs of alkaloid regulators in *Catharanthus roseus* and tobacco, and regulate production of SGAs in tomato. In transgenic tomato, overexpression and dominant suppression of JRE genes caused drastic changes in SGA accumulation and in the expression of genes for metabolic enzymes involved in the multistep pathway leading to SGA biosynthesis, including the upstream mevalonate pathway. Transactivation and DNA–protein binding assays demonstrate that JRE4 activates the transcription of SGA biosynthetic genes by binding to GCC box-like elements in their promoters. These JRE-binding elements occur at significantly higher frequencies in proximal promoter regions of the genes regulated by JRE genes, supporting the conclusion that JREs mediate transcriptional co-ordination of a series of metabolic genes involved in SGA biosynthesis.**

**Keywords:** Jasmonates • Steroidal glycoalkaloids • Tomato • Transcription factors.

**Abbreviations:** bHLH, basic helix–loop–helix; CaMV, *Cauliflower mosaic virus*; EAR, ERF-associated amphiphilic repression; EMSA, electrophoretic mobility shift assay; ERF, ethylene response factor; GAME, glycoalkaloid metabolism; GC-MS, gas chromatography–mass spectrometry; GFP, green fluorescent protein; GUS,  $\beta$ -glucuronidase; JA, jasmonate; JAZ, jasmonate ZIM-domain protein; JRE, jasmonate-responsive ERF; LC-QTOF-MS, liquid chromatography–quadrupole time-of-flight–mass spectrometry; MeJA, methyl jasmonate; ORCA3, octadecanoid-derivative responsive *Catharanthus* 3; qRT-PCR, quantitative reverse transcription–PCR; SGA, steroidal glycoalkaloid.

## Introduction

Plants have evolved multitudes of defense and adaptation mechanisms to survive in fluctuating environments. To ward off threats imposed by pathogens and pests, plants produce and accumulate toxic substances, including a diverse array of alkaloids, terpenoids and other metabolites with bioactive properties (Bednarek and Osbourn 2009). Although these plant-derived chemicals, or phytochemicals, are widely exploited by humans as valuable compounds, they are often unwanted in food crops because of adverse impacts on human health (Betz 1999). Accordingly, elimination or reduction of such phytochemicals is a critical aim in plant breeding. Complex metabolic pathways, encompassing precursor-supplying primary pathways and downstream specialized pathways, produce defense compounds. Tight regulation, often involving transcriptional co-ordination of structural genes, is required to ensure restrained implementation of these costly chemical defenses, which often impose burdens on growth and development in plants (Baldwin 1998).

Jasmonates (JAs) play central signaling roles in a wide range of plant resistance and developmental responses (Wasternack and Hause 2013), including the elicitation of defense chemical pathways. Indeed, methyl jasmonate (MeJA) has been widely used as an elicitor to induce the production of secondary metabolites in plant culture (Yukimune et al. 1996). Perception of JA signals and the subsequent signal transduction pathway steps, mediated by CORONATINE INSENSITIVE 1, JASMONATE ZIM-DOMAIN proteins (JAZs) and JAZ-interacting transcription factors, have been elucidated through molecular and genetic studies and are conserved among plant species (Wasternack and Hause 2013). However, less is known about the molecular mechanisms linking JA signaling with downstream defense-related metabolism (De Geyer et al. 2012). A group of JA-inducible ETHYLENE RESPONSE

FACTOR (ERF) transcription factors, categorized into clade 2 of group IXa (Nakano et al. 2006, Shoji et al. 2010, Shoji et al. 2013), have been found to play regulatory roles in JA-induced alkaloid biosynthesis in distinct species. For instance, OCTADECANOID-DERIVATIVE RESPONSIVE CATHARANTHUS 3 (ORCA3) controls the JA-dependent production of monoterpene indole alkaloids, including clinically important compounds, in the medicinal species *Catharanthus roseus* (van der Fits and Memelink 2000). Similarly, the JA-induced formation of ornithine-derived nicotine is regulated by ERF189 in tobacco (Shoji et al. 2010). Both ORCA3 and ERF189 mediate the co-ordinated transcription of a series of metabolic and transport genes (Shoji et al. 2009) involved in the alkaloid pathways by recognizing specific GCC box-like elements found in promoters of the target genes (van der Fits and Memelink 2000, Shoji et al. 2010, Shoji and Hashimoto 2011a). The JA-inducible expression of ORCA3 and ERF189 is regulated by a homolog of the basic helix–loop–helix (bHLH) family MYC2 transcription factor (Zhang et al. 2011, Shoji and Hashimoto 2011b). MYC2 is a JAZ-interacting factor, involved in the regulation of a wide range of downstream JA responses (Kazan and Manners 2013).

Steroidal glycoalkaloids (SGAs), which occur in certain species of Solanaceae and Lilaceae families, are nitrogen-containing compounds with a glycosylated steroidal backbone derived from cholesterol. Based on their cytotoxic properties, SGAs have been proposed to function in plant defense against biotic threats (Friedman 2002, Friedman 2006). SGAs are present as toxic and anti-nutritional compounds in inedible parts of solanaceous vegetables, such as immature green fruits of tomato and sprouts and green peels of potato tubers (Friedman 2002, Friedman 2006, Iijima et al. 2013). In tomato,  $\alpha$ -tomatine, derived from its aglycone tomatidine through elaborate glycosylation steps, is the predominant SGA in green organs, while its less toxic derivatives are found in red ripe fruits (Iijima et al. 2009). After early molecular studies on glycosyltransferases involved in the glycosylation (Moehs et al. 1997, Itkin et al. 2011), a series of GLYCOALKALOID METABOLISM (GAME) genes were identified as responsible for enzymatic steps from cholesterol to SGAs in tomato and potato (Itkin et al. 2013). STEROL SIDE CHAIN REDUCTASE 2 (SSR2) plays a key role in diverting the metabolic flow to cholesterol formation from cycloartenol (Sawai et al. 2014). Similar to other metabolic genes that form clusters in plant genomes (Boycheva et al. 2014), GAME genes are clustered in both the tomato and potato genomes (Itkin et al. 2013).

Cárdenas et al. (2016) recently identified five tomato ERF genes phylogenetically related to alkaloid-regulating ORCA3 and ERF189, and reported that one of them regulates the metabolic genes involved in the biosynthesis of SGAs in tomato and potato (Cárdenas et al. 2016). Here, we report characterization of these genes, which we term *Jasmonate-responsive ERF (JRE)* genes, as well as of a sixth related JRE in tomato. We performed transcript profiling and metabolite analyses of transgenic tomato lines with altered JRE function. We demonstrated that JRE genes play central roles in the transcriptional regulation of pathways leading to SGA formation, from the isoprenoid-supplying mevalonate pathway to GAME-mediated steps

after cholesterol. Transactivation and DNA–protein binding studies indicated that JRE4 positively controls the biosynthesis genes by recognizing GCC box-like elements in their promoters. Significant enrichment of putative JRE-binding elements in proximal 5'-flanking regions of JRE-regulated genes, including those involved in SGA biosynthesis, further supports the conclusion of JRE-mediated transcriptional co-ordination of these genes.

## Results

### Six JRE genes and their expression patterns in tomato

In tomato, there is a gene cluster (spanning about 100 kb) with five clade 2 ERF genes of group IXa on chromosome I (Cárdenas et al. 2016); we found that one additional ERF gene of this clade resides as a singleton on chromosome V (Fig. 1a). Since all six ERF genes were inducible by jasmonate (see below), we named them *Jasmonate-responsive ERF (JRE)* 1 (Soly01g090300), JRE2 (Soly01g090310), JRE3 (Soly01g090320), JRE4 (Soly01g090340), JRE5 (Soly01g090370) and JRE6 (Soly05g050790). Note that JRE1, JRE2, JRE3, JRE4 and JRE5, respectively, correspond to GAME9-like1, GAME9-like2, GAME9-like3, GAME9 and GAME9-like4 reported in a very recent study (Cárdenas et al. 2016).

Based on alignment of amino acid sequences of the conserved DNA-binding domain, a phylogenetic tree including JREs from tomato and related ERF proteins from *Arabidopsis*, *Catharanthus roseus* and tobacco was generated to examine the evolutionary relationships among the members (Fig. 1b). As defined previously (Shoji et al. 2013), clade 2 is divided into four subgroups. JRE3 and JRE4 were placed in clade 2–2b, and the remaining four JREs were in clade 2–3 (Fig. 1b).

We examined the expression patterns of JRE genes along with SGA biosynthetic *3-hydroxy-3-methylglutaryl CoA reductase (HMGR1)*, *sterol 4 $\alpha$ -methyl oxidase 2 (SMO2)* and GAME1 genes in tomato tissues using quantitative reverse transcription–PCR (qRT–PCR) (Fig. 2 and numerical values in Supplementary Table S1). Both JRE genes and SGA biosynthesis genes were expressed in organs from 7-week-old plants, and no apparent organ specificity was observed (Fig. 2a). JRE4 was the most highly expressed JRE in nearly all examined tissues, though in roots and fruits at certain stages the predominance of JRE4 was diminished, mainly due to decreased JRE4 expression in the tissues. The levels of toxic SGAs, such as  $\alpha$ -tomatine, as well as their production drastically decrease during fruit ripening in parallel with increased catabolism of toxic SGAs to less toxic forms (Iijima et al. 2009). In accordance with such changes, expression of SGA biosynthesis genes and some members of JRE genes, JRE1, JRE2 and JRE4, progressively decreased as fruits matured (Fig. 2b). Except for HMGR1, expression of which clearly declined at the breaker stage, decreases in the SGA biosynthesis and JRE gene expression were most evident during green fruit stages (Fig. 2b), when fruits were rapidly enlarging, rather than during later color-changing stages. Expression levels of JRE genes in cultured hairy roots were comparable with or

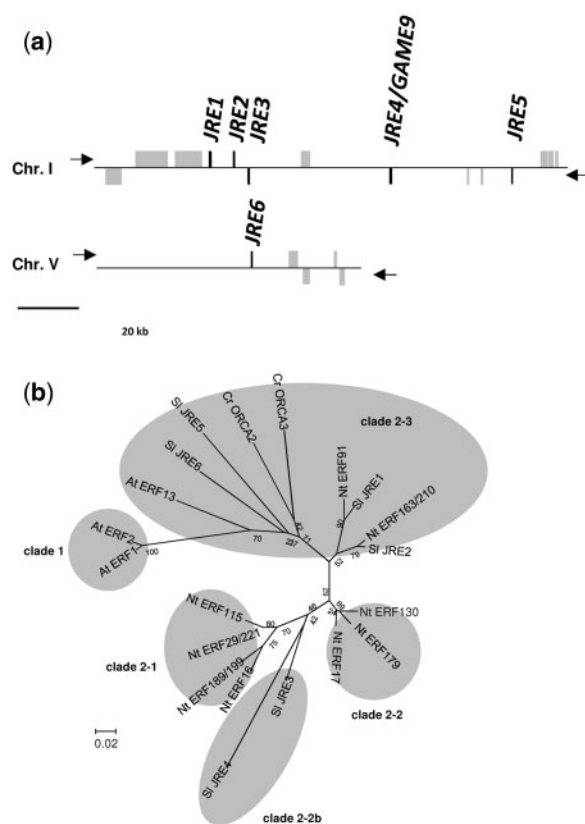


**Fig. 1** Tomato *JRE* genes. (a) Schematic presentation of the cluster of five *JRE* genes on chromosome I and *JRE6* on chromosome V. *JRE* and other genes are represented as black and gray boxes, respectively. Strands on which each gene resides are indicated with arrowheads. (b) Phylogenetic tree of tomato *JRE*s and related ERF proteins from Arabidopsis, *Catharanthus roseus* and tobacco. Two clade 1 ERF proteins of group IXa, AtERF1 and AtERF2, were included as an outgroup. Amino acid sequences of the DNA-binding domain were aligned using ClustalW (Thompson et al. 1994). An unrooted phylogenetic tree was constructed using the Neighbor-Joining algorithm with MEGA6 (Tamura et al. 2013). Bootstrap values are indicated at branch nodes, and the scale bar indicates the number of amino acid substitution per site. Species names are denoted with prefixes. At, Arabidopsis; Cr, *C. roseus*; Nt, tobacco; Sl, tomato.

somewhat higher than those in tissues from greenhouse-grown plants, suggesting the usefulness of the cultured material in studies on *JRE* genes and SGA biosynthesis. MeJA co-ordinately induced SGA biosynthesis genes in tomato hairy roots (Fig. 2c). All *JRE* genes were induced by MeJA treatment in tomato hairy roots, but the induction kinetics in terms of magnitude and timing varied among the members (Fig. 2c). *JRE4* and *JRE6* were gradually induced during the 24 h duration. Acute and strong induction within 30 min followed by a sharp decline was characteristic of *JRE1*, *JRE2* and *JRE3*. Induction of *JRE5* peaked at 4 h after the start of the treatment.

### Generation of transgenic tomato lines with altered function of *JRE* genes

To study the effect of altered *JRE* function on gene expression and metabolism in tomato, stable transgenic tomato lines of

plants and hairy roots were generated by *Agrobacterium*-mediated transformation. Two *JRE4* overexpression (*JRE4-OX*) lines of plants (lines OX1 and OX12) were established by introducing *JRE4* cDNA under the control of the *Cauliflower mosaic virus* (CaMV) 35S promoter. *JRE4* was chosen as a target gene for overexpression because it is the main *JRE* expressed in tomato tissues (Fig. 2). In leaves of the *JRE4-OX* lines, high expression of *JRE4* transcript was confirmed; this expression did not significantly change with MeJA treatment (Supplementary Fig. S1a). In contrast, MeJA induced the endogenous *JRE4* gene in wild-type controls (Supplementary Fig. S1a). No visible abnormalities were observed in the *JRE4-OX* plants (Supplementary Fig. S1b).

We chose a dominant suppression strategy to compromise *JRE* function, since the closely related *JRE* genes could have overlapping functions. For this purpose, *JRE3*, *JRE4* and *JRE5* were fused at their C-termini with the ERF-associated amphiphilic repression (EAR) motif, which dominantly suppresses expression of genes targeted by transcription factors (Hiratsu et al. 2003). The *JRE-EAR* genes were overexpressed using the CaMV 35S promoter in transgenic tomato hairy roots; two independent lines (lines #1 and #2) for each construct were selected and analyzed. Overexpression of the introduced *JRE* genes was confirmed in *JRE-EAR* lines using qRT-PCR (Supplementary Fig. S2). Consistent with different expression levels of the endogenous *JRE* genes (Fig. 2), the degrees of overexpression relative to vector controls varied among the lines with different fusion constructs. There was significant reduction of off-target *JRE* gene expression (e.g. *JRE1* and *JRE2* in all *JRE-EAR* lines, and *JRE6* in *JRE3-EAR* and *JRE5-EAR* lines) (Supplementary Fig. S2), suggesting down-regulation of the *JRE* genes by the *JRE-EAR* fusions. There were slight variations of growth and morphology among the lines (not shown), but they were within the range normally observed for hairy root cultures.

### Transcript profiling in overexpression and dominant suppression lines of *JRE* genes

To clarify the regulatory function of *JRE* transcription factors in tomato, we investigated the effects of altered *JRE* function on the transcriptome to reveal genes targeted by *JRE* genes. Comparative transcript profiling was carried out using the overexpression and dominant suppression transgenic lines with a custom tomato oligoarray representing >40,000 transcripts (Ruii et al. 2015). Total RNA from each line was labeled and hybridized to the array. As control samples for comparison, wild-type plants for overexpression and empty vector control lines for suppression were included. To examine the profiles in distinct types of tissues as well as after JA elicitation, leaves of *JRE4-OX* lines and hairy roots of suppression lines treated with MeJA were used for analysis.

Array oligos representing genes up-regulated in *JRE4-OX* lines and down-regulated in *JRE-EAR* lines are listed in Supplementary Tables S2 and S3, respectively; the list of the genes represented is given in Supplementary Table S4. A large number of metabolic genes involved in SGA biosynthesis were among the *JRE*-regulated genes; 24 genes regulated in either

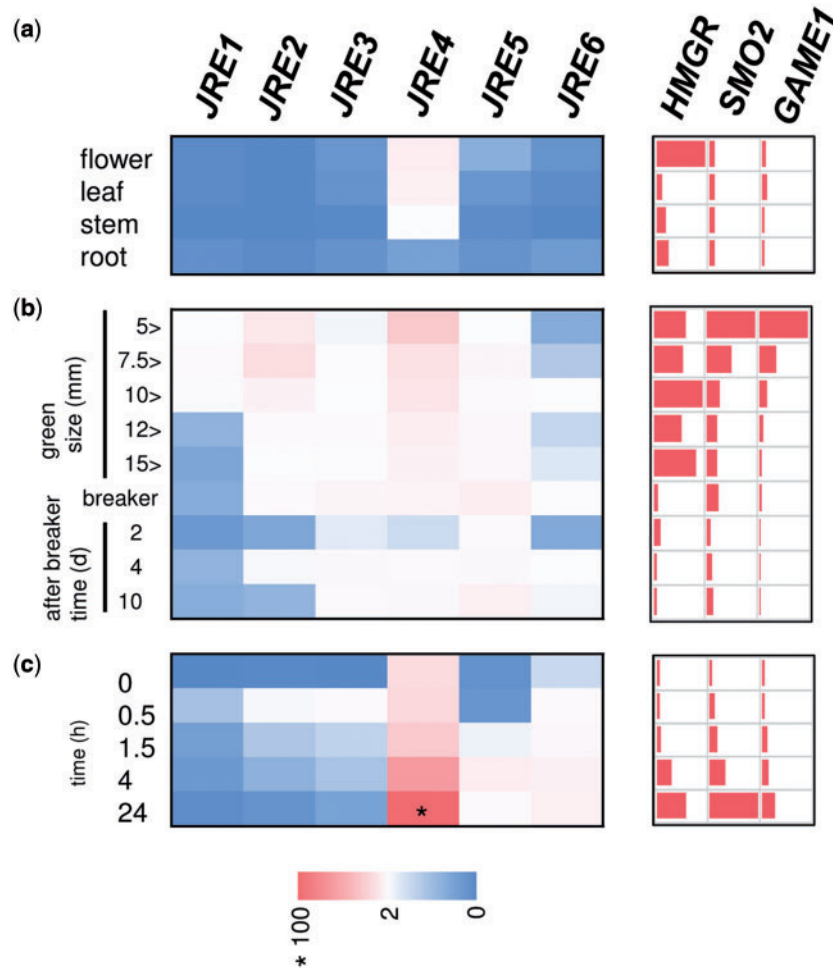


**Fig. 2** Expression patterns of *JRE* genes in tomato. Tomato flower, leaf, stem and root (a) and fruits of different ripening stages (b) were examined. Wild-type tomato hairy roots were treated with 100  $\mu$ M MeJA for 0, 0.5, 1, 4 and 24 h (c). Transcript levels were analyzed by qRT-PCR. Heat maps were drawn using average values (**Supplementary Table S1**) of three biological replicates. For *JRE* genes, values are calculated relative to those of *EF1 $\alpha$* , and are shown relative to the value (set to 100, marked with asterisk) of *JRE4* in hairy roots treated with MeJA for 24 h. For *HMGR1*, *SMO2* and *GAME1*, levels are shown relative to those in leaf, in fruit at stages with the highest expression for each, or in hairy roots at 0 h.

*JRE4-OX* or *JRE-EAR* lines (**Fig. 3**; **Supplementary Table S5**). All genes, except two (Soly05g055760 for *IDI* and Soly02g069490 for *SSR2*), whether they satisfied both listing criteria ( $R_{ox} > 5.0$ ,  $Q < 0.85$ ) or not, showed trends of signal increases in *JRE4-OX* lines as well as decreases in *JRE-EAR* lines. The *JRE*-regulated metabolic genes were involved in nearly all branches of the pathway leading to SGAs from the upstream mevalonate pathway to cholesterol biosynthesis and downstream aglycone formation and glycosylation (**Fig. 3**). The extent of regulation generally seemed greater for later steps, especially those after cholesterol (**Fig. 3**); *GAME* genes were especially responsive to alterations of *JRE* function (**Supplementary Tables S2, S3**). All of the biosynthesis genes were similarly suppressed by *JRE3-EAR*, *JRE4-EAR* and *JRE5-EAR*; this tendency was corroborated by the unbiased distribution of probes for SGA biosynthesis genes (**Supplementary Fig. S3**).

To validate the results of microarray analyses, transcript levels of SGA biosynthesis genes were analyzed in *JRE4-OX* and *JRE4-EAR* lines by qRT-PCR. Increased expression of the

genes, except *acetyl-CoA C-acetyltransferase* (*ACAA*), was observed in leaves of *JRE4-OX* lines relative to wild-type controls in both MeJA-treated and mock-treated conditions (**Fig. 4a**). Consistent with the microarray analysis results, the degree of up-regulation in *JRE4-OX* lines was greater for genes involved in later parts of the pathway (**Fig. 4a**). We also found clear up-regulation of *SMO2* and *GAME1* but not *HMGR1* of the mevalonate pathway in roots from *JRE4-OX* plants (**Supplementary Fig. S4**). In transgenic hairy roots expressing *JRE4-EAR*, all of the examined SGA biosynthesis genes were suppressed to 28–70% relative to the controls (**Fig. 4b**).

### Metabolic impact of altered *JRE4* function

To clarify how altered *JRE4* function affects SGA-related metabolism in tomato, we examined metabolite levels in leaves from *JRE4-OX* plants exposed to MeJA vapor (**Fig. 5a**) and hairy roots of a *JRE4-EAR* line treated with MeJA (**Fig. 5b**). SGAs, including the predominant  $\alpha$ -tomatine, were extracted and measured using liquid chromatography–quadrupole time-of-flight–mass



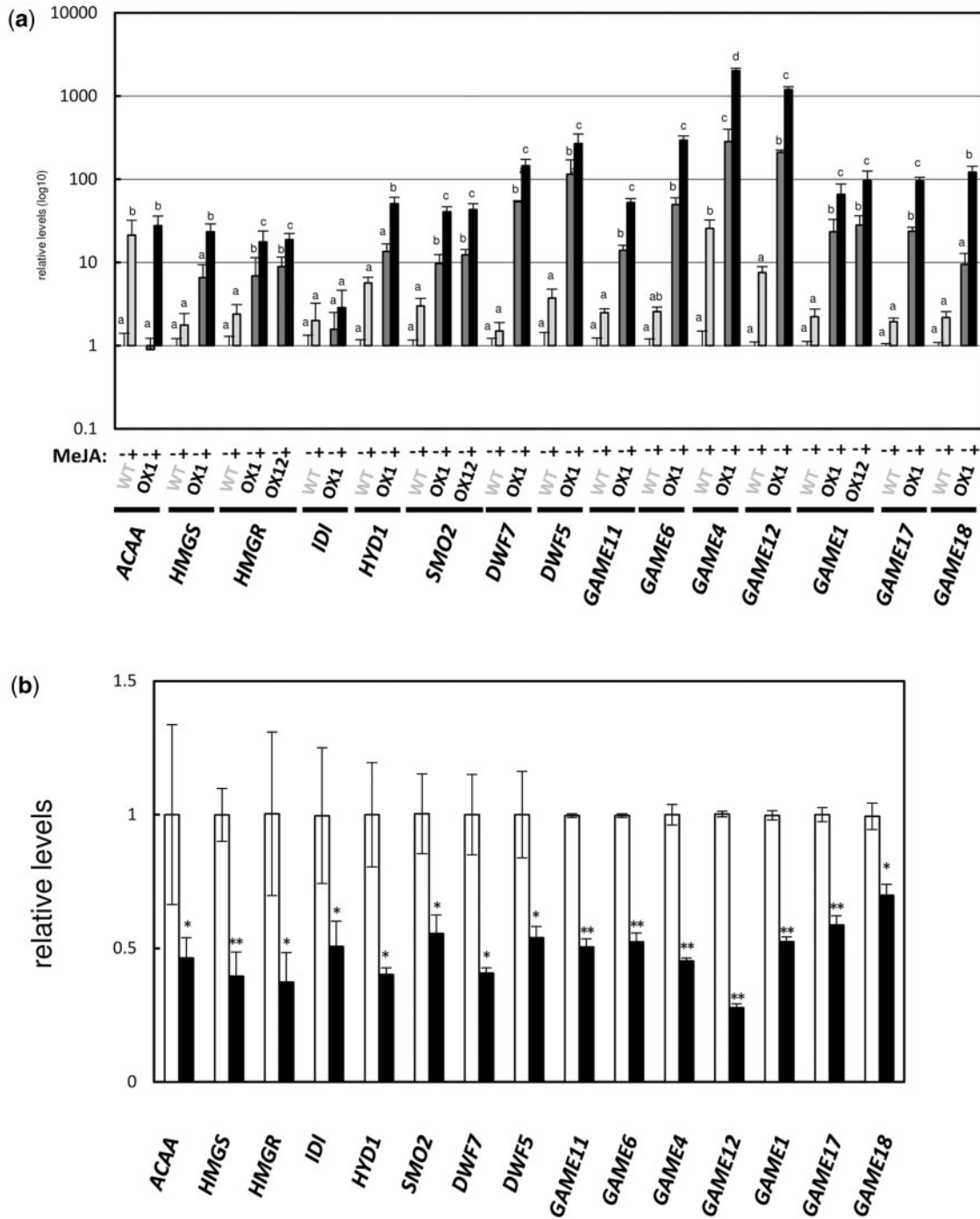


**Fig. 4** Expression levels of SGA biosynthesis genes in transgenic tomato *JRE4-OX* plant and *JRE4-EAR* hairy root lines. Transcript levels were analyzed by qRT-PCR. The error bars indicate the SD for three biological replicates. Levels are shown relative to the controls. See the legend of **Fig. 3** for abbreviations of gene names. (a) Levels in leaves from *JRE4-OX* plant lines treated with MeJA for 24 h. (b) Levels in hairy roots of *JRE4-EAR* (line #1) treated with MeJA for 24 h.

spectrometry (LC-QTOF-MS), whereas more hydrophilic substances, including pathway intermediates and other sterols and triperpenoids, were analyzed using gas chromatography–mass spectrometry (GC-MS). In the *JRE4-OX* line (line OX1), the level of  $\alpha$ -tomatine increased 2.1-fold relative to wild-type controls, while in the *JRE4-EAR* line (line #1), clear reductions of  $\alpha$ -tomatine to 47% the level of controls were observed. Similar changes

were observed for other SGAs (**Supplementary Table S6; Supplementary Fig. S5**). Cholesterol, a sterol precursor of SGAs, increased 1.5-fold in the *JRE4-EAR* line. The phytosterols campesterol and stigmasterol did not show any significant changes except for a 32% decrease of stigmasterol in the *JRE4-OX* line (**Fig. 5**). Cycloartenol and lanosterol, the first tetracyclic triperpenoid intermediates, were markedly decreased in

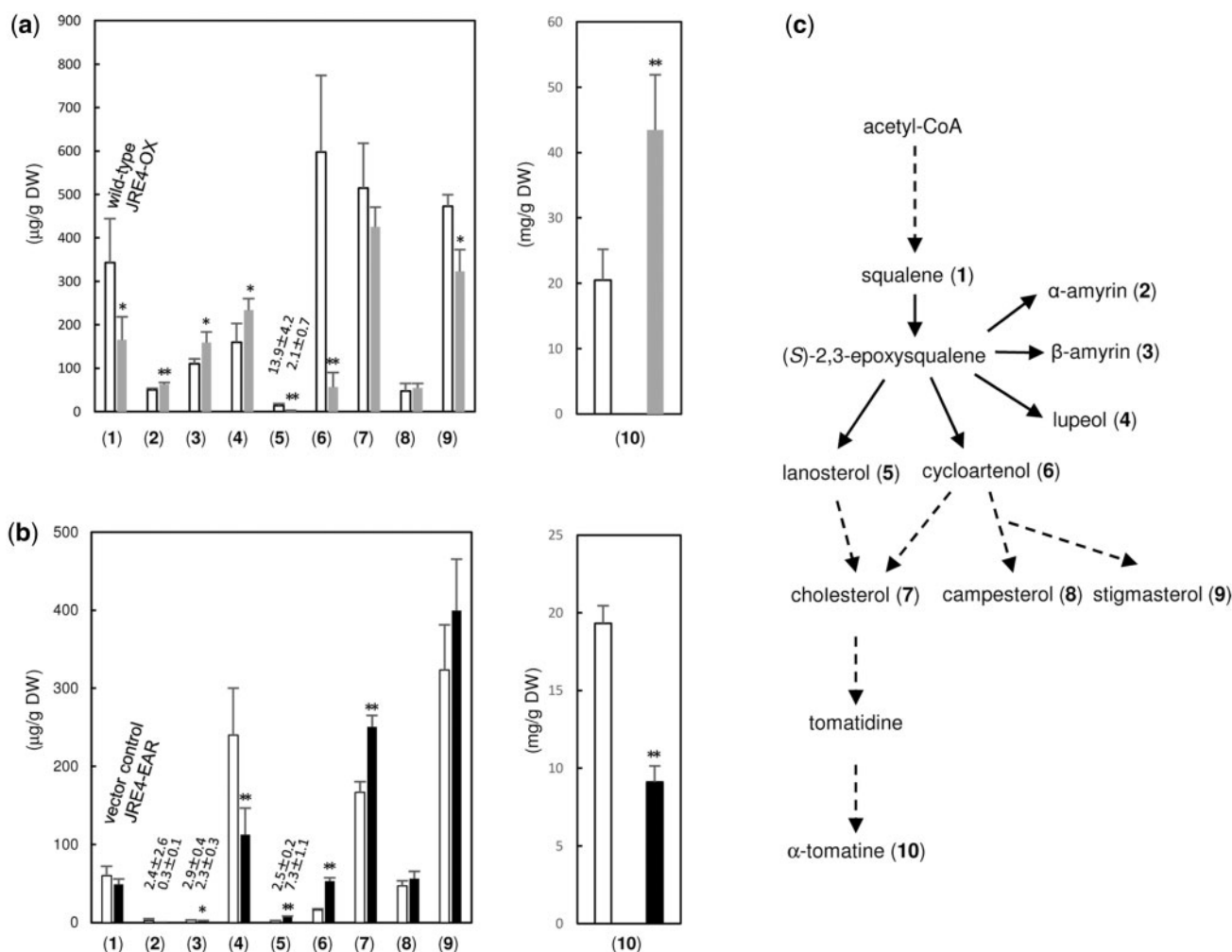


**Fig. 5** Metabolite levels in transgenic tomato *JRE4-OX* plants and *JRE4-EAR* hairy root lines. Metabolite levels were analyzed by LC-QTOF-MS for  $\alpha$ -tomatine and by GC-MS for other compounds. The error bars represent the SD from four (for a) or five (for b) biological replicates. Levels of other SGAs are available in [Supplementary Table S6](#). (a) Levels in leaves from *JRE4-OX* plants (line OX1) exposed to MeJA vapor for 4 d. (b) Levels in hairy roots of *JRE4-EAR* (line #1) treated with MeJA for 4 d. (c) Metabolites are schematically indicated in the SGA biosynthesis pathway.

the *JRE4-OX* line, to 9% and 15% of levels in the control, respectively, while a 3.3-fold increase of cycloartenol and a 2.9-fold increase of lanosterol were observed in the *JRE4-EAR* line. Triterpenoids, namely  $\alpha$ -amyryn,  $\beta$ -amyryn and lupeol, were increased 1.3- to 1.5-fold in the *JRE4-OX* line and decreased to 14–80% of the control levels in the *JRE4-EAR* line. Squalene decreased to 48% of the level in the control in the *JRE4-OX* line and did not significantly change in the *JRE4-EAR* line.

### JRE4 activates transcription of SGA biosynthesis genes by binding to GCC box-like promoter elements

To examine whether JRE4 activates the transcription of SGA biosynthesis genes in vivo through their 5' -flanking regions, transient transactivation assays were performed in tomato fruits using *Agrobacterium*-mediated infection, or agroinjection, for gene delivery. For transient expression, the  $\beta$ -glucuronidase (*GUS*) reporter was placed downstream of the 5'-flanking region of *sterol reductase* (*DWF5*) (−1,500 to −1;

counted from the first ATG) or *GAME4* (−1,500 to −1) ([Fig. 6a](#)). The individual reporter constructs and a CaMV 35S promoter-driven *JRE4* effector were co-delivered into tomato fruits by agroinjection along with a CaMV 35S promoter-driven *green fluorescent protein* (*GFP*) reference construct. The expression levels of the *GUS* reporter genes were analyzed by qRT-PCR and normalized to that of the reference *GFP* gene ([Fig. 6b](#)). *DWF5* and *GAME4* promoter-driven *GUS* reporter genes were up-regulated 3.8- and 8.2-fold by *JRE4* overexpression, respectively, indicating that the *JRE4*-mediated gene activation was dependent on regions included in the reporter constructs. The 1,500 bp region of *DWF5* could be trimmed to a relatively short span (−285 to −1) without losing reporter responsiveness (10.6-fold) ([Fig. 6b](#)) and basal activity, indicating the functional importance of this proximal region.

*JRE4* recognizes two structurally related elements, the GCC box-like P box and the GCC box (Shoji et al. 2013; [Supplementary Table S7](#)). Accordingly, we used in silico analysis to identify P box and GCC box elements within the

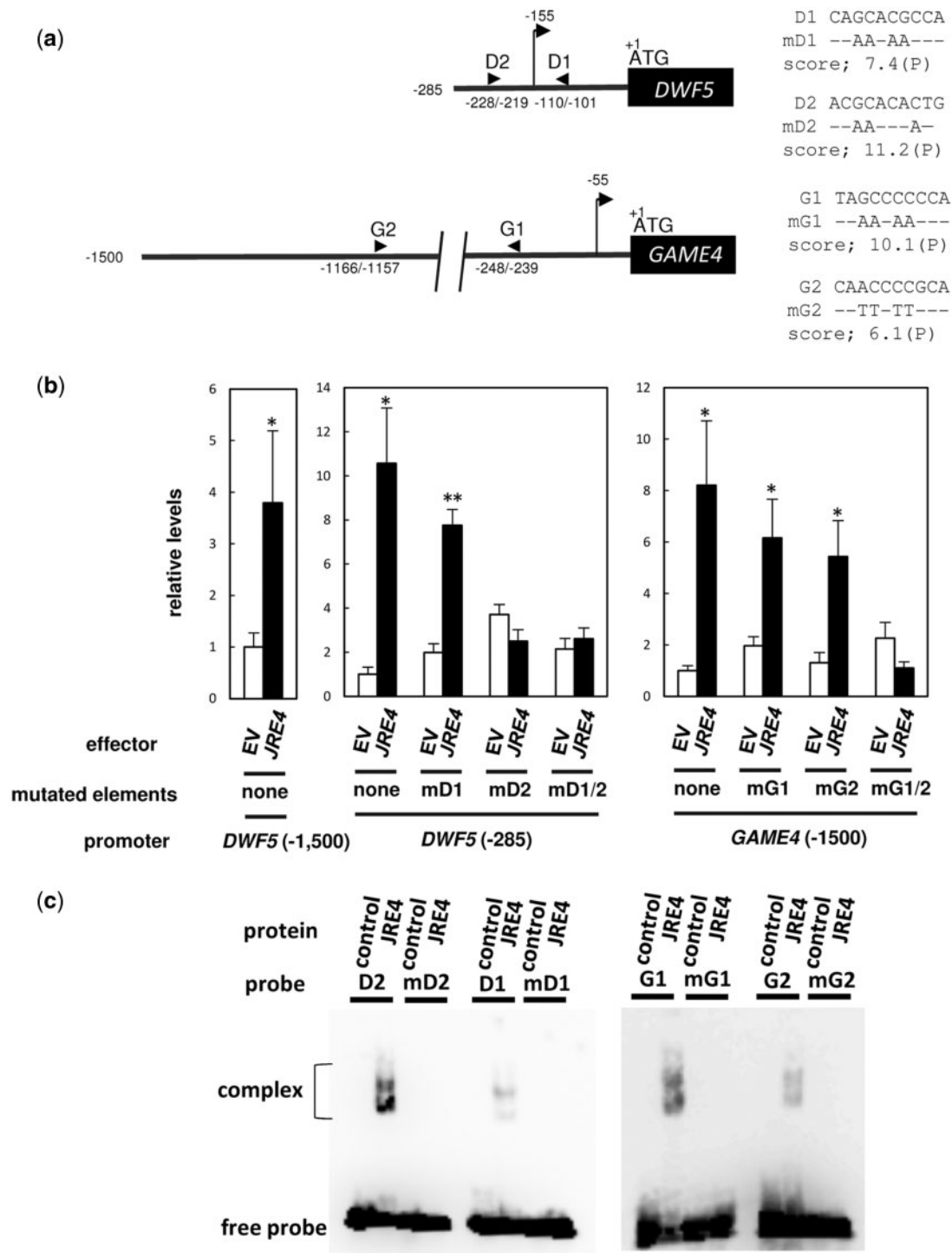


**Fig. 6** *JRE4*-mediated activation of *DWF5* and *GAME4* is dependent on *JRE*-binding elements found in the promoter regions. (a) Schematic representation of 5'-flanking regions of *DWF5* and *GAME4*. The positions of *JRE*-binding elements (arrowheads) and transcriptional start sites (arrows with vertical lines) are shown. On the right, nucleotide sequences of the elements are shown, while only the substituted nucleotides are indicated in mutated versions. (b) Transient transactivation assays in tomato fruits. The *GUS* reporter gene, fused with 5'-flanking regions of *DWF5* (−1,500 to −1 or −285 to −1; counted from the first ATG) and *GAME4* (−1,500 to −1) or their mutated versions, was delivered into tomato fruits by agroinjection with *JRE4* effector plasmid or empty vector (EV) and *GFP* reference plasmid. Expression levels of the *GUS* reporter gene were normalized to those of the *GFP* reference gene, and are shown as relative values against the values of each wild-type reporter with EV. The bars indicate the SD from four independent experiments. Significant differences between EV and *JRE4* effector for each reporter were determined by Student's *t*-test: \**P* < 0.05; \*\**P* < 0.01. (c) EMSA showing in vitro binding of recombinant *JRE4* to the predicted elements. Probes were incubated with proteins from EV control or recombinant *JRE4*. Probe sequences are available in [Supplementary Table S10](#).



1,500 bp 5'-flanking regions of *DWF5* and *GAME4*. Using a cut-off score of 7.0, two P boxes (named D1 and D2) in *DWF5* and one P box (named G1) encompassing a GCC box in *GAME4* were predicted, while no GCC box, other than the one included in G1, was found. Both D1 and D2 were present within the short functional region (−285 to −1) of *DWF5*.

To clarify the role of the predicted elements in the *JRE4*-dependent reporter activation, nucleotides within the elements were substituted (Fig. 6a) and the resultant mutant reporters were subjected to transient transactivation assays (Fig. 6b). For *DWF5*, mutations in D1 abolished the *JRE4*-dependent activation of the reporter driven by the short region (−285 to −11). Mutations in D2, which resides in the 5'-untranslated region rather than the promoter, did not have major influences on the induction, indicating the requirement for a functional D1 element but not for D2. *GAME4* promoter activation did not change much with mutations only in G1, suggesting the presence of additional elements indispensable for the promoter induction. Based on such an assumption, we lowered the cut-off value in the analysis, and found the G2 element (−1,111 to −1,102) with a score of 6.1 as a predicted P box (Fig. 6a). Mutations in G2 alone did not change activation, similar to those in G1 (Fig. 6b). However, when the *GAME4* promoter construct carried mutations at both G1 and G2, it was no longer activated by the *JRE4* effector, pointing to the involvement of functionally redundant G1 and G2 in the *GAME4* activation.

To validate in vitro binding of the elements to *JRE4* proteins, electrophoretic mobility shift assay (EMSA) was carried out with oligonucleotide probes based on sequences of the elements (Supplementary Table S10). When incubated with recombinant fusion proteins of truncated *JRE4* (corresponding to amino acids 40–219) tagged with N-terminal thioredoxin and other short tags, DNA–protein complexes were detected as intense shifted triplet bands for D2 and G1 probes (Fig. 6c). Similar patterns of shifted bands were observed for D1 and G2, albeit with lower intensity than those for the other two probes. Interestingly, the intensities of the shifted bands corresponded to the in silico prediction scores for the elements. The shifted bands were completely abolished when mutated probes (Fig. 6a) were used, confirming the specificity of binding of the wild-type probes.

### Putative *JRE*-binding elements found in proximal promoter regions of *JRE*-regulated genes

The *JRE4*-binding elements found in proximal promoter regions (Fig. 6) prompted us to examine whether genes with such *JRE*-binding elements in promoter regions were enriched among *JRE*-regulated genes. In addition to the P and GCC boxes targeted by clade 2–2b *JRE4*, a related CS1 box, recognized by clade 2–3 *JREs* (Fig. 7a), was included in the analysis. All of the examined boxes were represented as weighted matrices (Supplementary Table S7). We computationally searched for P, GCC and CS1 boxes with a cut-off score of 7.0 in promoter regions (up to −800; counted from the first ATG) of *JRE*-regulated genes (group R) (180 genes in Supplementary Table S4) and of *JRE*-regulated SGA biosynthesis genes (group SR) (24 genes in Fig. 3), a subset of group R genes. The corresponding

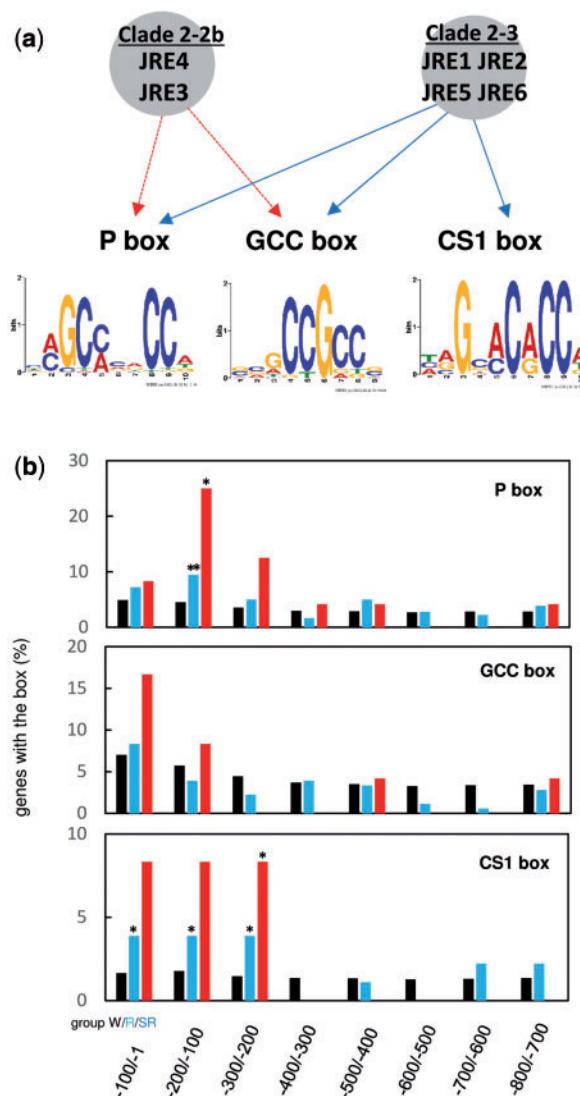


**Fig. 7** Computational prediction of putative *JRE*-binding elements in promoter regions of genes regulated by *JRE* genes. (a) Presumed binding elements of *JREs*. DNA-binding specificities of *JRE4* and related ERFs from other species had been studied (Shoji et al. 2013); the binding of *JRE4* to P and GCC boxes was experimentally validated, while those for other *JREs* are presumed based on the results of clade 2–2b *JRE4* for *JRE3* and those of clade 2–3 ORCA3 from *C. roseus* for the remaining four *JREs*. Sequence logos representing P, CS1 and GCC boxes were generated by WebLogo (Crooks et al. 2004) based on position-specific probability matrices (Supplementary Table S7), which were determined using the sequences predicted in the 5'-flanking regions (−300 to −1) of group R genes. (b) Genes predicted with *JRE*-binding elements (scores >7.0) for the indicated region in groups W (black), R (blue) and SR (red). The genes of group R (180 *JRE*-regulated genes) and of group SR (*JRE*-regulated 24 SGA biosynthesis genes) are given in Supplementary Table S4 and in Fig. 3, respectively. Significant differences of values (shown in %) from those for group W (all 34,725 protein-coding genes in the tomato genome) were determined by one-sided Fisher's exact test; \**P* < 0.05, \*\**P* < 0.01.

regions of all protein-coding genes annotated in a tomato reference genome (group W) (34,725 genes) were analyzed as controls. The genes with the *JRE*-binding elements in each group were counted. The values even for group W were slightly

variable among examined regions, possibly reflecting biased GC contents or other genomic features in promoter regions. We detected enrichment of genes with a P box in the  $-200$  to  $-100$  region for both R (2.1-fold) and SR groups (5.8-fold) and of genes with a CS1 box in the  $-300$  to  $-1$  region for group R (2.2- to 2.7-fold) and in the  $-300$  to  $-200$  region for group SR (5.7-fold).

To examine whether sequences related to P, GCC and CS1 boxes could be retrieved in non-targeted analysis, the 5'-flanking sequences ( $-1,500$  to  $-1$ ) of group R and SR genes were subjected to MEME (Multiple EM for Motif Elicitation) analysis (Bailey et al. 2006), retrieving the sequences shared among the queries. Multiple sequences with similarity to the JRE-binding boxes were retrieved (Supplementary Table S8); match scores representing the similarities were calculated using position-specific probability matrices for P, GCC and CS1 boxes based on sequences retrieved from the 5'-flanking regions ( $-300$  to  $-1$ ) of group R genes (Supplementary Table S7).

## Discussion

### Impacts of altered JRE function on SGA biosynthesis

Here, we used transgenic approaches, involving overexpression and dominant suppression, to elucidate the regulatory functions of tomato JRE transcription factors, which are closely related to alkaloid-regulating ORCA3 from *C. roseus* (van der Fits and Memelink 2000) and ERF189 from tobacco (Shoji et al. 2010). Based on microarray analyses, we identified a large number of JRE-regulated metabolic genes involved in SGA biosynthesis, including all clustered GAME genes except GAME2, constituting a core pathway downstream of cholesterol (Itkin et al. 2011, Itkin et al. 2013), genes for cholesterol biosynthesis, including SSR2 (Sawai et al. 2014) and flux-controlling HMGR (Narita and Grussem 1989), and others involved in the mevalonate pathway (Fig. 2). Our results demonstrate the existence of JRE-mediated transcriptional regulation of the entire SGA pathway in tomato. This regulation of the upstream pathways, as far up as the isoprenoid-producing branch, may be required to meet the metabolic demands for downstream SGA production without disturbing homeostasis of other metabolites derived from the highly branched terpenoid pathways. The relatively small changes in the accumulation of the essential phyosterols (Boutté and Grebe 2009) campesterol and stigmaterol in the transgenic lines support this conclusion (Fig. 4). Although the overall pathway to SGA biosynthesis was generally co-ordinated, expression levels of genes involved in later steps, such as GAME genes, changed much more in the transgenic lines than did the upstream genes (Figs. 3, 4a; Supplementary Fig. S4; Supplementary Tables S2, S3, S5). Such differential regulation between distinct parts of the pathway was corroborated with the changes in the levels of metabolites; changes in SGAs and upstream intermediates, cholesterol, cycloartenol, lanosterol and squalene, showed opposite trends in both the overexpression and the suppression lines (Fig. 5). This difference in accumulation presumably

reflects imbalances between the early and late parts of the pathway. To understand the metabolic changes of triterpenoids,  $\alpha$ -amyirin,  $\beta$ -amyirin and lupeol, which showed a trend opposite to that of cycloartenol and lanosterol (Fig. 5), it might be useful to examine the regulation of *oxidosqualene cyclase* genes, none of which was identified as a regulated gene in our microarray analysis. Of course, to better understand the metabolic impacts of JRE4 overexpression, we need to examine not only the expression of the metabolic genes at the transcript level but also activities of the involved enzymes and metabolic flux reflecting them.

Our microarray-based approach to screening genes involved in a JRE-controlled regulon not only points to known structural genes (Fig. 3) but also helps mine novel metabolic and transport genes required for complex SGA-related metabolism. In this regard, it is intriguing that many uncharacterized genes annotated as encoding glucosyltransferases, Cyt P450 enzymes and peptide transporters were included in the list of JRE-regulated genes (Supplementary Table S4). Similar transgenic approaches combined with transcript profiling in other species producing SGAs are considered useful to elucidate the molecular bases of chemically diverse metabolites of this group (Friedman 2002, Friedman 2006, Iijima et al. 2013). It should be noted that Cárdenas et al. (2016) recently reported that potato GAME9, an ortholog of tomato GAME9/JRE4, regulates the biosynthetic genes of the SGAs chaconine and solanine (Cárdenas et al. 2016). Our identification of a series of JRE-regulated metabolic genes in tomato provides new insights on cholesterol formation, which has been relatively unexplored in plants compared with other organisms (Sawai et al. 2014).

To understand this regulation in the context of a greater metabolic network, we will need to address the co-ordination of the JRE-mediated transcriptional regulation with other mechanisms operating at the transcriptional and post-transcriptional levels (Pollier et al. 2013, Mertens et al. 2015, Van Moerkercke et al. 2015). As discussed below, it is still an open question whether all parts of the pathway are similarly subjected to the transcriptional regulation by JRE genes. In addition to structural genes, molecular factors important for the regulation of the pathway could be included in the JRE-regulated genes. Notably, among the genes identified as regulated by JRE genes (Supplementary Table S4) was a gene encoding a RING-finger E3 ubiquitin ligase, a homolog of MAKIBISH1 from *Medicago truncatula* that controls HMGR enzyme activity (Pollier et al. 2013). Studies of tomato JRE genes and GAME9 (Cárdenas 2016; this study), along with recent studies on a group of related bHLH transcription factors (Van Moerkercke et al. 2015, Mertens et al. 2015), open a new chapter in the study of the regulation of terpenoid pathways, which had remained unexplored until recently.

### Transcriptional regulation of SGA biosynthesis genes

JRE4 directly activates the transcription of DWF5 and GAME4 genes by recognizing the GCC-like elements in their promoter regions (Fig. 6). Two of the three functional elements found in DWF5 and GAME4 are present in similarly situated proximal

regions (−248 to −219 relative to the ATG) (**Fig. 6a**). This finding is consistent with previous reports on ORCA3- and ERF189-recognizing elements present in similar regions of the targeted genes (Van der Fits and Memelink 2000, Shoji et al. 2010, Shoji and Hashimoto 2011a) and also with the computational predictions of the elements in the *JRE*-regulated genes (**Fig. 7**), suggesting a common mechanistic feature among transcription factors of this group. Our results for *GAME4*, which is present in a two-gene metabolic cluster (**Fig. 6**), point to a role for promoter-binding transcription factors in the regulation of such clusters, possibly in addition to their proposed regulation at the chromosomal level (Wegel et al. 2009).

It remains to be addressed whether all *JRE*-regulated SGA biosynthesis genes, including clustered *GAME* genes other than *GAME4*, are regulated directly by *JRE* genes in a similar manner to that demonstrated for *DWF5* and *GAME4*. Considering the large number of regulated steps and the differential regulation we observed, we cannot exclude the possibility of the involvement of additional mechanisms, such as indirect regulation through other transcription factors or metabolite-mediated feedback regulation. As demonstrated for regulation of nicotine biosynthesis genes by ERF189 and the JAZ-interacting bHLH transcription factor MYC2 (Shoji and Hashimoto 2011b), it is also plausible that JREs regulate the downstream genes in cooperation with other transcription factors. In this regard, it is interesting that both MYC2 and *GAME4/JRE4* were required for transactivation of promoters of SGA biosynthesis genes in tobacco cells (Cárdenas et al. 2016). Nevertheless, the significant enrichment among the *JRE*-regulated genes of those bearing a P or CS1 box in the proximal promoter (**Fig. 7**) and the complementary results of the MEME analysis (**Supplementary Table S8**) suggest that *JRE4*, and possibly other JREs, including clade 2–3 members that can recognize the CS1 box, participate in the transcriptional regulation of many, but not necessarily all, of the genes by binding to the predicted elements. The frequent occurrence of the *JRE*-binding elements in the regulated genes supports the notion that genes acting downstream are recruited into regulons under the control of transcription factors through acquisition of functional *cis*-elements in the appropriate promoter regions (Shoji and Hashimoto 2011a, Moghe and Last 2015).

The results of our promoter-related analyses (**Figs. 6, 7; Supplementary Table S8**) point to the possible importance of GCC-like P and CS1 boxes rather than the canonical GCC box for *JRE*-mediated regulation, although all JREs presumably have substantial abilities to bind to GCC boxes *in vitro* (**Fig. 7a**, Shoji et al. 2013). As proposed for tobacco ERF189, which exclusively targets the P box (Shoji et al. 2013), such a preference for the GCC-like box of JREs may allow the *JRE*-controlled regulon to be free from influence by the large number of GCC box-recognizing ERFs.

### Regulatory function of multiple *JRE* genes

Gene clustering is common to *JRE* genes (**Fig. 1a**) and related *ERF* genes (Shoji et al. 2013); in tobacco, *ERF189* is clustered with related genes on a nicotine-controlling *NIC2* locus, and the *NIC2*-locus cluster was found to be deleted in a low-nicotine

mutant (Shoji et al. 2010), while *ORCA3* was found to reside on the same genomic contig with a similar gene in *C. roseus* (Kellner et al. 2015). When overexpressed in a low-nicotine mutant, *ERF189* recovered nicotine accumulation to the wild-type levels, and thus *ERF189* has been considered to work most effectively as a regulator of nicotine biosynthesis among the clustered *ERF* genes (Shoji et al. 2010). Similar to the *NIC2*-locus cluster in tobacco, the tomato *JRE* cluster includes members of different clades, namely clades 2–2b and 2–3 (**Fig. 1**). Dominant suppression of clade 2–2b *JRE3*, 2–2b *JRE4* or 2–3 *JRE5* similarly repressed the expression of SGA biosynthesis genes (**Fig. 3; Supplementary Fig. S3**), suggesting overlapping functions of the three *JRE* genes. Of course, the effects of ectopic expression of the dominant repressive forms of these proteins should be interpreted carefully. The involvement of clade 2–3 *JRE* genes in SGA regulation is also supported by the frequent occurrences of CS1 boxes in promoters of the regulated genes. In addition to overexpression (**Fig. 3; Supplementary Fig. S4; Supplementary Table S2**) and promoter binding (**Fig. 6**) analyses as performed herein for *JRE4*, knock-out or knock-down experiments for individual members would be required to confirm the *in planta* contributions of each *JRE* gene to SGA regulation.

The gene expression patterns strongly support a role for *JRE4* in SGA regulation (**Fig. 2**). *JRE4* is expressed the most highly among *JRE* genes at the transcript level and, as pointed out in Itkin et al. (2013), its expression is clearly co-ordinated with SGA biosynthesis genes in various samples (**Fig. 2**). In fruits, progressive decreases of expression were evident for *JRE4*, *SMO2* and *GAME1* during the green fruit stages (**Fig. 2b**), indicating that SGA formation mainly declines during the green stages rather than later color-changing stages (Iijima et al. 2009). In hairy roots, all *JRE* genes were clearly induced by MeJA treatment, but their induction patterns were variable between the members (**Fig. 2c**). Again, the gradual induction of *JRE4* paralleled those of SGA biosynthesis genes during the 24 h duration of treatment. According to the co-expression analysis and other evidence, we can infer that one or a few select members, such as tomato *JRE4*, tobacco *ERF189* and possibly *C. roseus* *ORCA3*, play a predominant role in regulation of targeted metabolic pathways in each species. We need to understand further the functional redundancy and divergence among the multiple *ERF* members to address why these *ERF* genes are maintained in a form of gene clusters during plant evolution.

### SGAs as defense chemicals in tomato

Plants usually adapt particular classes of metabolites for chemical defense. A variety of compounds, including SGAs, methyl ketones and sesquiterpenes, are considered to mediate the herbivore resistance in *Solanum* species (Antonious et al. 2014). SGAs are a group of bioactive compounds with abilities to bind to cholesterol, disrupt cellular membranes and inhibit cholinesterases (Friedman 2015). Based on their toxic and pharmacological properties, SGAs have been proposed to be involved in plant host resistance against a wide range of biotic agents, such as bacteria, fungi, viruses, insects and animals (Friedman 2002, Friedman 2006). A series of genes encoding

biosynthetic enzymes and transcription factors involved in SGA biosynthesis were induced by MeJA treatment in tomato tissues (Figs. 2c, 4a; Supplementary Figs. S1, S4). The JA-induced expression of the genes and involvement of tomato homologs of ORCA3 and ERF189 in their induction underline the committed roles of SGAs and JA signaling in induced chemical defense against herbivores in tomato, as in the case of nicotine in tobacco (Baldwin 1998, Shoji and Hashimoto 2013). Although induced significantly after elicitation, SGAs and nicotine are substantially produced even at basal levels and the amounts of SGA and nicotine accumulation in the tissues seem to be in a similar range (in the order of  $\text{mg g}^{-1}$  DW), indicating the similarities of these two alkaloid groups with analogous regulatory mechanisms. Drastic declines of expression of SGA biosynthetic and regulatory JRE genes during early fruit development in tomato (Fig. 2c) are an example of developmental regulation of defense chemical pathways, which may operate more generally, ensuring the removal of toxic substances from seed-bearing mature fruits to allow seed dispersal assisted by fruit-eating herbivores.

One of the main goals in tomato and potato breeding is the removal of toxic and anti-nutritional SGAs, which are not critically required for plant protection during normal cultivation and occasionally cause poisoning. The removal of SGAs becomes critical when considering the introduction of desirable genetic traits into cultivated species from wild counterparts that usually produce SGAs at higher levels (Iijima et al. 2013). Our identification of the transcriptional regulators of the SGA pathway provides a promising molecular tool applicable for the generation of the crops with low SGA contents.

## Materials and Methods

### Plant growth, transformation and treatment

Sterilized seeds of tomato, *Solanum lycopersicum* cv. Micro-Tom, were germinated and grown to seedlings on half-strength Gamborg B5 medium solidified with 0.6% (w/v) agar and supplemented with 2% (w/v) sucrose. Two-week-old seedlings were transferred onto soil in pots and grown to maturity in the greenhouse.

The coding region of JRE4 was cloned into the BamHI and SacI sites on pBI121 to generate a binary vector p35S::JRE4 for overexpression. The p35S::JRE4 vector was introduced into *Agrobacterium tumefaciens* strain GV2260 by electroporation. *Agrobacterium*-mediated transformation to generate transgenic tomato plants was done according to Sun et al. (2006). Shoots were selected on solidified Murashige and Skoog medium containing  $100 \text{ mg l}^{-1}$  kanamycin. Diploid individuals were screened in the T<sub>0</sub> generation. Transgenic plants of the T<sub>3</sub> generation were analyzed.

For gene expression analyses, leaves and roots from 4-week-old plantlets grown in a greenhouse were submerged in B5 medium with  $100 \mu\text{M}$  MeJA and incubated for 24 h in the dark. Four individual 7-week-old plants were placed in air-tight plastic containers (approximately 81 liters in volume), with a cotton sheet soaked with 5 ml of  $100 \mu\text{M}$  MeJA. The cotton sheet was replaced with a newly soaked one every day during the duration of treatment. Leaves detached from plants exposed to MeJA vapor for 4 d were used for metabolite analysis.

To generate the dominant suppression vectors, coding sequences of JRE3, JRE4 and JRE5 were amplified by PCR with primers including the restriction sites and a sequence for the EAR motif (5'-CGGCCGCTTGATTTGGATCTTGAAGCTCAGACTTGGATTTGCTTA-3'; encoding LDLLELRGFA; Hiratsu et al., 2003) and inserted into the XbaI and SacI sites of pBI121. To generate transgenic hairy roots, tomato hypocotyls from 7-day-old seedlings were infected with

*Agrobacterium rhizogenes* strain ATCC15834 harboring a binary vector by briefly touching one end of a hypocotyl segment (1.5 cm in length) to a bacterial colony and then standing the segments on the same agar medium with the contacted end up. Hairy roots emerging from infected sites were excised and subcultured twice every week on solidified B5 medium containing  $300 \text{ mg l}^{-1}$  cefotaxime for disinfection and  $50 \text{ mg l}^{-1}$  kanamycin for drug resistance selection. The selected lines were maintained by subculturing every week in 125 ml glass flasks filled with 25 ml of liquid B5 medium supplemented with 2% (w/v) sucrose with shaking at 100 r.p.m. in the dark. MeJA was directly added to 4-day-old cultures to a final concentration of  $100 \mu\text{M}$ .

### cDNA microarray analysis

Total RNA was isolated from leaves treated with MeJA for 24 h and hairy roots treated with MeJA for 24 h using an RNeasy kit (Qiagen). RNA integrity was checked with an Agilent 2100 Bioanalyzer (Agilent). Total RNA (500 ng) was used to generate Cyanine 3-labeled cRNA probes using a Quick Amp Labeling Kit, One-Color (Agilent). A tomato custom oligoarray with 60-mer probes of >40,000 sequences, designed using transcript sequences of the Tomato Gene Index Version 11 (LeGI v.11; <http://www.danarfarber.org/>), was hybridized with the labeled samples and scanned, and data were captured and processed as described (Ruii et al. 2015). Due to poor labeling, hybridization was cancelled for the sample from JRE4-EAR line #2.

Probes with low signal intensity (averages for the two controls <0.2) and variable intensities between lines (differences between the two controls >2.5-fold) were excluded from the analysis. Values relative to the controls were obtained by pairwise comparisons and averaged for each construct; values were defined as  $R_{ox}$ ,  $R_{j3}$ ,  $R_{j4}$  and  $R_{j5}$  derived from data for JRE4-OX, JRE3-EAR, JRE4-EAR and JRE5-EAR lines, respectively. For the overexpression experiment, probes with  $R_{ox} > 5$  are listed in Supplementary Table S2. For the suppression experiment, Q was defined as  $Q^2 = R_{j3}^2 + R_{j4}^2 + R_{j5}^2$ , and probes with  $Q < 0.85$  are listed in Supplementary Table S3.

### qRT-PCR

Total RNA was isolated from plant samples that had been ground in liquid nitrogen using an RNeasy kit (Qiagen) and then converted to first-strand cDNA using ReverTra Ace qPCR RT Master Mix (Toyobo) with oligo(dT) primer. The cDNA templates were amplified using a LightCycler 96 (Roche) with SYBR Premix Ex Taq (Takara) according to Shoji et al. (2010). The primer sequences are given in Supplementary Table S9. EF1 $\alpha$  (SolyC05g005060) was used as a reference gene. Each assay was repeated at least three times. Based on amplifications from equal molar quantities of cloned amplicons, amplifications from different primer pairs were normalized.

### Metabolite analysis

For measurement of SGAs, freeze-dried samples (2 mg) were extracted with 250  $\mu\text{l}$  (for hairy root samples) or 500  $\mu\text{l}$  (for leaf samples) of 80% (v/v) methanol containing 2.5  $\mu\text{M}$  lidocaine and 2.5  $\mu\text{M}$  10-camphor sulfonic acid using a mixer mill with zirconia beads for 7 min at 18 Hz and 4 °C. After centrifugation for 10 min at  $12,000 \times g$ , the supernatant was filtered using an HLB  $\mu\text{Elution}$  plate (Waters). The extracts (1  $\mu\text{l}$ ) were analyzed using LC-QTOF-MS (LC, Waters Acquity UPLC system; MS, Waters Xevo G2 Q-ToF). Positive ion mode was used and analytical conditions were as follows: LC column, acuity bridged ethyl hybrid (BEH) C18 (1.7  $\mu\text{m}$ , 2.1 mm  $\times$  100 mm, Waters); solvent system, solvent A (water including 0.1% formic acid) and solvent B (acetonitrile including 0.1% formic acid); gradient program, 99.5% A/0.5% B at 0 min, 99.5% A/0.5% B at 0.1 min, 20% A/80% B at 10 min, 0.5% A/99.5% B at 10.1 min, 0.5% A/99.5% B at 12.0 min, 99.5% A/0.5% B at 12.1 min and 99.5% A/0.5% B at 15.0 min; flow rate, 0.3 ml  $\text{min}^{-1}$  at 0 min, 0.3 ml  $\text{min}^{-1}$  at 10 min, 0.4 ml  $\text{min}^{-1}$  at 10.1 min, 0.4 ml  $\text{min}^{-1}$  at 14.4 min and 0.3 ml  $\text{min}^{-1}$  at 14.5 min; column temperature, 40 °C; MS detection: capillary voltage, +3.0 keV, cone voltage, 25.0 V, source temperature, 120 °C, desolvation temperature, 450 °C, cone gas flow, 50 l  $\text{h}^{-1}$ ; desolvation gas flow, 800 l  $\text{h}^{-1}$ ; collision energy, 6 V; mass range,  $m/z$  50–1,500; scan duration, 0.1 s; inter-scan delay, 0.014 s; data acquisition, centroid mode; Lockspray (leucine enkephalin): scan duration, 1.0 s; inter-scan delay, 0.1 s. MS/MS data were acquired in ramp mode using the following analytical conditions: (i) MS: mass range,  $m/z$  50–1,500; scan duration,

0.1 s; inter-scan delay, 0.014 s; data acquisition, centroid mode; polarity, positive/negative; and (ii) MS/MS: mass range,  $m/z$  50–1,500; scan duration, 0.02 s; inter-scan delay, 0.014 s; data acquisition, centroid mode; polarity, positive/negative collision energy, ramped from 10 to 50 V. In this mode, MS/MS spectra of the top 10 ions (> 1,000 counts) in an MS scan were automatically obtained. If the ion intensity was < 1,000, MS/MS data acquisition was not performed and moved to the next top 10 ions. Chemical assignment of SGAs was performed using the MS/MS spectra reported in Itkin et al. (2011). All SGA levels were calculated based on a calibration curve of  $\alpha$ -tomatine (Tokyo Chemical Industry Co., Ltd.), assuming the same molar responses of SGAs.

For measurement of triterpenes, the extraction of plant tissues with added standards ([25,26,26,27,27,27- $^2\text{H}_7$ ]cholesterol (98% D, Cambridge Isotope Laboratories, Inc.) or synthesized [3,28,28,28- $^2\text{H}_4$ ] $\beta$ -amyirin, [28,28,28- $^2\text{H}_3$ ] $\alpha$ -amyirin and 28,28,28- $^2\text{H}_3$ ]lupeol; Ohyama et al. 2007) was carried out using the method previously described (Tsukagoshi et al. 2016). Quantification of triterpenes except for lanosterol and squalene using GC-MS analysis was performed as described previously (for sterols, Choi et al. 2014; for triterpenols, Ohyama et al. 2007). Lanosterol amounts were calculated using the peak area ratio of the fragment ion ( $m/z$ : 393) of trimethylsilylated lanosterol and that ( $m/z$ : 336) of the standard (TMS derivative of the labeled cholesterol). Quantification of squalene was performed using the standard calibration curve with coefficients of determination,  $r^2 > 0.9996$ . The curves were constructed using the peak area value of TIC (total ion chromatogram).

## Transactivation assay

The 5'-flanking regions of *DWF5* and *GAME5* were amplified by PCR from tomato genomic DNA with primers attached to the restriction sites and cloned into the *HindIII* and *BamHI* sites on pBI121 to generate the *GUS* reporter constructs. For mutant reporter constructs, before cloning the fragments into pBI121, PCR-based mutagenesis (Hemsley et al. 1989) was used to substitute the nucleotides in the cloned promoter sequences; nucleotide substitutions introduced are shown in Fig. 6a. *pGBW17* was used as the empty vector control for the effector plasmids. The binary vectors, *p19s* for P19 silencing suppressor (Voinnet et al. 2003) and *p35S-GFP* for the *GFP* reference gene, were used.

Transient gene expression was performed in tomato fruits according to an agroinjection protocol (Orzaez et al. 2006). Briefly, *Agrobacterium tumefaciens* strain EHA105 with a binary vector was grown overnight in YEB medium supplemented with 20  $\mu\text{M}$  acetosyringone and appropriate antibiotics, and recovered by centrifugation at 4,000  $\times g$  for 20 min. The cells were re-suspended in infiltration buffer (10 mM MES, 10 mM  $\text{MgCl}_2$ , 200  $\mu\text{M}$  acetosyringone, pH 5.7) by adjusting the optical density at 600 nm to 0.25, and then incubated for at least 2 h at room temperature in the dark. The bacterial suspensions for reporter and effector vectors plus those for *p19s* and *p35S-GFP* vectors were combined, and the resultant solution (200–300  $\mu\text{l}$  per fruit) was injected into mature green fruits (1–1.5 cm in size) using a 1 ml plastic syringe attached to a 27-gauge needle. Gene expression was analyzed by qRT-PCR using fruits harvested 3 d after the injection.

## EMSA

Bacterial expression and purification of recombinant fusion proteins of JRE4, called S11g90340 in Shoji et al. (2013), were done as described (Shoji et al. 2013). In the pET32b-based expression vector, a portion of *JRE4* (corresponding to amino acid residues 40–219) was placed downstream of a sequence for N-terminal tags, a thioredoxin, an S-tag and a His-tag (Shoji et al. 2013). Proteins comprising only the tag portion from empty pET32b were purified and used as the controls.

Sequences of sense and antisense oligonucleotides used are given in **Supplementary Table S10**. Probe preparation, DNA–protein binding assays, gel separation and detection of the reaction products were carried out as described (Shoji et al. 2010).

## Computational analysis

We used Regulatory Sequence Analysis Tools (RSAT; Turatsinze et al. 2008, <http://rsat.ulb.ac.be/rsat/>) to search for putative JRE-binding elements in the query genomic sequences by weight matrix scoring. Weight matrices for the P, GCC and CS1 boxes (Shoji et al. 2013) are given in **Supplementary Table S7**.

The default settings were used for all parameters. Elements with scores higher than 7.0 were retained for analysis, along with element G2, which had a score of 6.1 in *GAME4*. Genes with putative JRE-binding elements in the examined regions were counted. Significant differences of the values compared with those of group W including all tomato protein-coding genes was determined by one-sided Fisher's exact test ( $\alpha = 0.05$ ) using the Fisher test function of R (V. 3.2.2).

Based on sequences predicted to be the JRE-binding elements by RSAT in the regions (–300 to –1) of group R genes, position-specific probability matrices for P, GCC and CS1 boxes (**Supplementary Table S7**) were generated by MEME software (v. 4. 10. 2., Bailey et al. 2006) with option settings; '2' for '-nmotif', '10' for '-minw' and applying '-revcomp'. To retrieve the sequences commonly found in the queries, MEME was used with option settings; '10' for '-nmotif', '7' for '-minw' and applying '-revcomp'. Match scores representing the similarities between a pair of the retrieved sequence and the JRE-binding box (P, GCC or CS1) were calculated using position-specific probability matrices for the pairs. When a pair of sequences with lengths of  $L_1$  and  $L_2$  were aligned with the overlapping length of  $L_3$ , the alignment length  $L_e$  was defined as  $L_e = L_1 + L_2 - L_3$ . Differences between 1 and normalized vector distances were summed for overlapping positions and divided by  $L_e$  to give scores for the alignments. The alignment scores were calculated for all possible alignments with no gap in both orientations for a sequence pair, and the highest alignment score was adapted as a match score for the pair.

## Supplementary data

Supplementary data are available at PCP online.

## Funding

This work was supported by the Japan Society for the Promotion of Science [a Grant-in-Aid for Scientific Research (C) (grant No. 26440144 to T.S.)]; the Plant Transgenic Design Initiative, Gene Research Center, University of Tsukuba [a Cooperative Research Grant]; RIKEN Plant Transformation Network; the Japan Advanced Plant Science Network.

## Acknowledgements

We thank Drs. Tsuyoshi Nakagawa and Yoshinori Yagi for providing *pGBW17* and *p35S-GFP*, respectively.

## Disclosures

The authors have no conflicts of interest to declare.

## References

- Antonious, G.F., Kamminga, K. and Snyder, J.C. (2014) Wild tomato leaf extracts for spider mite and cowpea aphid control. *J. Environ. Sci. Health B*. 49: 527–531.
- Bailey, T.L., Williams, N., Misleh, C. and Li, W.W. (2006) MEME: discovering and analyzing DNA and protein sequence motifs. *Nucleic Acids Res.* 34: W369–W373.
- Baldwin, I.T. (1998) Jasmonate-induced responses are costly but benefit plants under attack in native populations. *Proc. Natl. Acad. Sci. USA* 95: 8113–8118.
- Bednarek, P. and Osbourn, A. (2009) Plant–microbe interactions: chemical diversity in plant defense. *Science* 324: 746–748.
- Betz, J.M. (1999) Plant toxins. *J. AOAC Int.* 82: 781–784.

- Boutté, Y. and Grebe, M. (2009) Cellular processes relying on sterol function in plants. *Curr. Opin. Plant Biol.* 12: 705–713.
- Boycheva, S., Daviet, L., Wolfender, J.L. and Fitzpatrick, T.B. (2014) The rise of operon-like gene clusters in plants. *Trends Plant Sci.* 19: 447–459.
- Cárdenas, P.D., Sonawane, P.D., Pollier, J., Bossche, R.V., Dewangan, V., Weithorn, E., et al. (2016) GAME9 regulates the biosynthesis of steroidal alkaloids and upstream isoprenoids in the plant mevalonate pathway. *Nat. Comm.* 7: 10654.
- Choi, H., Ohyama, K., Kim, Y.Y., Jin, J.Y., Lee, S.B., Yamaoka, Y., et al. (2014) The role of Arabidopsis ABCG9 and ABCG31 ATP binding cassette transporters in pollen fitness and the deposition of steryl glycosides on the pollen coat. *Plant Cell* 26: 310–324.
- Crooks, G.E., Hon, G., Chandonia, J.M. and Brenner, S.E. (2004) WebLogo: a sequence logo generator. *Genome Res.* 14: 1188–1190.
- De Geyter, N., Gholami, A., Goormachtig, S. and Goossens, A. (2012) Transcriptional machineries in jasmonate-elicited plant secondary metabolism. *Trends Plant Sci.* 17: 349–359.
- Friedman, M. (2002) Tomato glycoalkaloids: role in the plant and in the diet. *J. Agric. Food Chem.* 50: 5751–5780.
- Friedman, M. (2006) Potato glycoalkaloids and metabolites: roles in the plant and in the diet. *J. Agric. Food Chem.* 54: 8655–8681.
- Friedman, M. (2015) Chemistry and anticarcinogenic mechanisms of glycoalkaloids produced by eggplants, potatoes, and tomatoes. *J. Agric. Food Chem.* 63: 3323–3337.
- Hemsley, A., Amheim, N., Toney, M.D., Cortpassi, G. and Galas, D.J. (1989) A simple method for site-directed mutagenesis using the polymerase chain reaction. *Nucleic Acids Res.* 17: 6547–6551.
- Hiratsu, K., Mitsuda, N., Matsui, K. and Ohme-Takagi, M. (2003) Dominant repression of target genes by chimeric repressors that include the EAR motif, a repression domain, in Arabidopsis. *Plant J.* 34: 733–739.
- Iijima, Y., Fujiwara, Y., Tokita, T., Ikeda, T., Nohara, T., Aoki, K., et al. (2009) Involvement of ethylene in the accumulation of esculeoside A during fruit ripening of tomato (*Solanum lycopersicum*). *J. Agric. Food Chem.* 57: 3247–3252.
- Iijima, Y., Watanabe, B., Sasaki, R., Takenaka, M., Ono, H., Sakurai, N., et al. (2013) Steroidal glycoalkaloid profiling and structures of glycoalkaloids in wild tomato fruit. *Phytochemistry* 95: 145–157.
- Itkin, M., Heinig, U., Tzfadia, O., Bhide, A.J., Shinde, B., Cardenas, P., et al. (2013) Biosynthesis of antinutritional alkaloids in Solanaceous crops is mediated by clustered genes. *Science* 341: 175–179.
- Itkin, M., Rogachev, I., Alkan, N., Rosenberg, T., Malitsky, S., Masini, L., et al. (2011) GLYCOALKALOID METABOLISM1 is required for steroidal alkaloid glycosylation and prevention of phytotoxicity in tomato. *Plant Cell* 23: 4507–4525.
- Kazan, K. and Manners, J.M. (2013) MYC2: the master in action. *Mol. Plant* 6: 686–703.
- Kellner, F., Kim, J., Clavijo, B.J., Hamilton, J.P., Childs, K.L., Vaillancourt, B., et al. (2015) Genome-guided investigation of plant natural product biosynthesis. *Plant J.* 82: 680–692.
- Mertens, J., Pollier, J., Vanden Bossche, R., Lopez-Vidriero, I., Franco-Zorrilla, J.M. and Goossens, A. (2016) The bHLH transcription factors TSAR1 and TSAR2 regulate triterpene saponin biosynthesis in *Medicago truncatula*. *Plant Physiol.* 170: 194–210.
- Moehs, C.P., Allen, P.V., Friedman, M. and Belknap, W.R. (1997) Cloning and expression of solanidine UDP-glucose glucosyltransferase from potato. *Plant J.* 11: 227–236.
- Moghe, G.D. and Last, R.L. (2015) Something old, something new: conserved enzymes and the evolution of novelty in plant specialized metabolism. *Plant Physiol.* 169: 1512–1523.
- Nakano, T., Suzuki, K., Fujimura, T. and Shinshi, H. (2006) Genome-wide analysis of the ERF gene family in Arabidopsis and rice. *Plant Physiol.* 140: 411–432.
- Narita, J.O. and Grissem, W. (1989) Tomato hydroxymethylglutaryl-CoA reductase is required early in fruit development but not during ripening. *Plant Cell* 1: 181–190.
- Ohyama, K., Suzuki, M., Masuda, K., Yoshida, S. and Muranaka, T. (2007) Chemical phenotypes of the *hmg1* and *hmg2* mutants of *Arabidopsis* demonstrate the in-planta role of HMG-CoA reductase in triterpene biosynthesis. *Chem. Pharm. Bull.* 55: 1518–1521.
- Orzaez, D., Mirabel, S., Wieland, W.H. and Granell, A. (2006) Agroinjection of tomato fruits. A tool for rapid functional analysis of transgenes directly in fruit. *Plant Physiol.* 140: 3–11.
- Pollier, J., Moses, T., González-Guzmán, M., De Geyter, N., Lippens, S., Vanden Bossche, R., et al. (2013) The protein quality control system manage plant defence compound synthesis. *Nature* 504: 148–152.
- Ruiu, F., Picarella, M.E., Imanishi, S. and Mazzucato, A. (2015) A transcriptomic approach to identify regulatory genes involved in fruit set of wild-type and parthenocarpic tomato genotypes. *Plant Mol. Biol.* 89: 263–278.
- Sawai, S., Ohyama, K., Yasumoto, S., Seki, H., Sakuma, T., Yamamoto, T., et al. (2014) Sterol side chain reductase 2 is a key enzyme in the biosynthesis of cholesterol, the common precursor for toxic steroidal glycoalkaloids in potato. *Plant Cell* 26: 3763–3774.
- Shoji, T. and Hashimoto, T. (2011a) Recruitment of a duplicated primary metabolism gene into the nicotine biosynthesis regulon in tobacco. *Plant J.* 67: 949–959.
- Shoji, T. and Hashimoto, T. (2011b) Tobacco MYC2 regulates jasmonate-inducible nicotine biosynthesis genes directly and by way of the NIC2-locus ERF genes. *Plant Cell Physiol.* 52: 1117–1130.
- Shoji, T. and Hashimoto, T. (2013) Smoking out the masters: transcriptional regulators for nicotine biosynthesis in tobacco. *Plant Biotechnol.* 30: 217–224.
- Shoji, T., Inai, K., Yazaki, Y., Sato, Y., Takase, H., Shitan, N., et al. (2009) Multidrug and toxic compound extrusion-type transporters implicated in vacuolar sequestration of nicotine in tobacco roots. *Plant Physiol.* 149: 708–718.
- Shoji, T., Kajikawa, M. and Hashimoto, T. (2010) Clustered transcription factor genes regulate nicotine biosynthesis in tobacco. *Plant Cell* 22: 3390–3409.
- Shoji, T., Mishima, M. and Hashimoto, T. (2013) Divergent DNA-binding specificities of a group of ETHYLENE RESPONSE FACTOR transcription factors involved in plant defense. *Plant Physiol.* 162: 977–990.
- Sun, H.J., Uchii, S., Watanabe, S. and Ezura, H. (2006) A highly efficient transformation protocol for Micro-Tom, a model cultivar for tomato functional genomics. *Plant Cell Physiol.* 47: 426–431.
- Tamura, K., Stecher, G., Peterson, D., Fillipski, A. and Kumar, S. (2013) MEGA6: molecular evolutionary genetic analysis version 6.0. *Mol. Biol. Evol.* 30: 2725–2729.
- Thompson, J.D., Higgins, D.G. and Gibson, T.J. (1994) CLUSTAL W: improving the sensitivity of progressive multiple sequence alignment through sequence weighting, position-specific gap penalties and weight matrix choice. *Nucleic Acids Res.* 22: 4673–4680.
- Tsukagoshi, Y., Suzuki, H., Seki, H., Muranaka, T., Ohyama, K. and Fujimoto, Y. (2016) *Ajuga*  $\Delta^{24}$ -sterol reductase catalyzes the direct reductive conversion of 24-methylenecholesterol to campesterol. *J. Biol. Chem.* 291: 8189–8198.
- Turatsinze, J.V., Thomas-Collier, M., Defrance, M. and van Helden, J. (2008) Using RSAT to scan genome sequences for transcription factor binding sites and cis-regulatory modules. *Nat. Protoc.* 3: 1578–1588.
- Van der Fits, L. and Memelink, J. (2000) ORCA3, a jasmonate-responsive transcriptional regulator of plant primary and secondary metabolism. *Science* 289: 295–297.
- Van Moerkercke, A., Steensma, P., Schweizer, F., Pollier, J., Gariboldi, I., Payne, R., et al. (2015) The bHLH transcription factor B1S1 controls the iridoid branch of the monoterpenoid indole alkaloid pathway in *Catharanthus roseus*. *Proc. Natl. Acad. Sci. USA* 112: 8130–8135.
- Voinnet, O., Rivas, S., Mestre, P. and Baulcombe, D. (2003) An enhanced transient expression system in plants based on suppression of gene silencing by the p19 protein of tomato bushy stunt virus. *Plant J.* 33: 949–956.

- Wasternack, C. and Hause, B. (2013) Jasmonates: biosynthesis, perception, signal transduction and action in plant stress response, growth and development. An update to the 2007 review in *Annals of Botany*. *Ann. Bot.* 111: 1021–1058.
- Wegel, E., Koumproglou, R., Shaw, P. and Osbourn, A. (2009) Cell type-specific chromatin decondensation of a metabolic gene cluster in oats. *Plant Cell* 21: 3926–3936.
- Yukimune, Y., Tabata, H., Higashi, Y. and Hara, Y. (1996) Methyl jasmonate-induced overproduction of paclitaxel and baccatin III in *Taxus* cell suspension cultures. *Nat. Biotechnol.* 14: 1129–1132.
- Zhang, H., Hedhili, S., Montiel, G., Zhang, Y., Chatel, G., Pré, M., et al. (2011) The basic helix–loop–helix transcription factor CrMYC2 controls the jasmonate-responsive expression of the ORCA genes that regulate alkaloid biosynthesis in *Catharanthus roseus*. *Plant J.* 67: 61–71.